Int. J. Heat Mass Transfer. Vol. 7, pp. 1051–1068. Pergamon Press 1964. Printed in Great Britain

LATENT HEAT TRANSPORT IN SATURATED NUCLEATE BOILING

C. J. RALLIS† and H. H. JAWUREK‡
Department of Mechanical Engineering,
University of the Witwatersrand, Johannesburg, South Africa

(*Received* 4 *December* 1963 *and in revised form* 15 *April* 1964)

Abstract—Experimental work on the nucleate pool boiling of water at saturation is reported. This indicates that latent heat transport, $(q/A)_{LH}$, is at all stages significant. The ratio $(q/A)_{LH}/(q/A)_{Tot}$ increases steadily with increasing heat flux and appears to tend to unity as $(q/A)_{Tot}$ tends towards burnout. Latent heat transport and convection together account for the total flux in saturated boiling.

The basic parameters entering into the formulation of $(q/A)_{LH}$, that is, the product of bubble frequency and bubble volume at departure—$f V_d$, and the bubble source concentration—N, are further investigated.

It is shown that most published findings on the parameter $f V_d$ are inapplicable to heat-transfer correlations due to the incorrect definition of means. Experimental results show that (i) the (arithmetic) mean product $\overline{f V_d}$ increases with flux, and (ii) at a particular flux the product $f V_d$ is approximately the same for each bubble source.

The data for N on water and on organics boiling at various pressures indicate that the relation

$$(q/A) = \text{constant} \cdot N^n$$

where $n \simeq 0{\cdot}5$ appears to hold only in the region of isolated bubbles.

A hypothesis is evolved and confirmed experimentally according to which the curve of N vs ΔT_{sat} takes the form of a cumulative frequency distribution.

Analysis and confirmatory experiments show that nucleation and nucleate boiling cannot be made to proceed indefinitely at lower and lower pressures; for a particular surface–liquid combination a pressure exists which marks the threshold of a hitherto unrecognized regime of unstable nucleate boiling. At lower pressures the nucleate regime is altogether absent.

NOMENCLATURE

a, constant;
A, heat-transfer area [ft²];
b, constant;
c, C, constants;
D_d, equivalent spherical bubble diameter at departure [ft];
f, bubble frequency [s^{-1} or h^{-1}];
f_i, bubble frequency of individual source [s^{-1} or h^{-1}];
$\bar{f}$, mean (arithmetic, unless otherwise stated) of f_i;
$\overline{f V_d}$, arithmetic mean of products $f_i V_{di}$;
g, gravitation acceleration [ft/h²];
G_d, mass velocity of vapour in departing bubbles [lb_m/h ft²];
m, constant;
n, constant;
n, number of bubble sources on heat-transfer surface;
$N = n/A$, bubble source concentration [ft^{-2}];
$\mathcal{N}$, nucleation site concentration [ft^{-2}];
Nu, Nusselt number;
P_L, liquid pressure [atm];
Pr, Prandtl number;
Q_b, enthalpy of formation of bubble [Btu];
(q/A), $(q/A)_{Tot}$, total heat flux [Btu/h ft²];
$(q/A)_{LH}$, latent heat transport, defined by equation (2) [Btu/h ft²];
$(q/A)_{NC}$, natural convection flux [Btu/h ft²];
r, nucleation cavity mouth radius [ft];
r_{max}, mouth radius of largest potentially active cavity [ft];

† Professor of Fluid Mechanics.
‡ South African Atomic Energy Board Bursar.

H.M.—3R

r^*_{max}, mouth radius of largest active cavity [ft];
r^*_{min}, mouth radius of smallest active cavity [ft];
Re, Reynolds number;
T_{sat}, saturation temperature of liquid [°R];
T_w, heater wall temperature [°R];
ΔT_{sat}, $(T_w - T_{sat})$ [degR];
V_b, bubble volume [ft^3];
V_d, bubble volume at departure [ft^3];
V_{di}, bubble volume at departure for a particular source [ft^3];
$\bar{V}_d$, mean (arithmetic, unless otherwise stated) of V_{di};
v_v, specific volume of vapour [ft^3/lb$_m$];

Greek symbols

δ, limiting thermal boundary layer thickness [ft];
λ_v, latent heat of vaporization [Btu/lb$_m$];
ρ_v, ρ_L, vapour and liquid density [lb$_m$/ft^3];
σ, surface tension [lb$_f$/ft].

1. INTRODUCTION

1.1 *Definition of latent heat transport*

This paper deals primarily with the transport of energy away from a heating surface associated with the formation of bubbles thereon during saturated nucleate pool boiling.

It has been shown [1, 2] that the energy Q_b required to form a bubble of volume V_b and of radius larger than about 10^{-7} ft, is given, to a good approximation, by

$$Q_b = V_b \rho_v \lambda_v \qquad (1)$$

with properties evaluated at the saturated state corresponding to the liquid pressure.

Since the diameter of bubbles at the instant of departure from a heated surface exceeds 10^{-7} ft by several orders of magnitude, the energy carried away from such a surface by bubbles may be formulated as

$$(q/A)_{LH} = \rho_v \lambda_v \sum_{i=1}^{n} f_i V_{di}/A \qquad (2)$$

Evidently equation (1) only represents the latent heat of formation of a bubble, other terms being negligible. Thus the flux contribution given by equation (2) is termed *latent heat transport*.

Inasmuch as our ultimate aim is the correlation of nucleate boiling heat fluxes, the choice of V_d, the bubble volume at the instant of departure from the heating surface, is the only logical one. It has been shown by Jakob [3], and is verified in the present study (at least for the case of low-flux boiling), that bubbles in saturated boiling continue to grow after departure until they reach the free liquid surface. The heat required for this growth must originally have left the heating surface by some convection mechanism, and must be correlated on that basis.

It is further accepted that the bulk of the heat required for *attached* bubble growth must also be transferred from the heating surface, via the liquid sub-layer, by some conduction/convection process. Evidently the ebullition mechanism is invoked and becomes rate controlling, when the normal convection processes tend to "saturation" and are no longer able to cope with the rate of heat supply. The exact distribution of heat flow between these two possible paths, that is convection and ebullition, clearly will be flux-dependent. It therefore appears preferable to correlate the flux contribution of the heat of formation of attached bubbles separately and in terms of equation (2).

To sum up therefore: The latent heat transport defined by equation (2) accounts for the heat that leaves the surface by conduction and convection to form bubbles up to the point of their departure; the difference between the total flux and the latent heat transport represents the heat that leaves the surface by convection, thereafter to manifest itself partly in the further growth of rising bubbles and partly in evaporation without ebullition at the free liquid surface.

1.2 *Previous work on latent heat transport*

It has until recently been generally held that in nucleate boiling, whether sub-cooled or saturated, latent heat transport as defined above contributes insignificantly to the total heat flux. This notion appears to have been based on the sub-cooled boiling studies of Gunther and Kreith [4] and Rohsenow and Clark [1].

As a result the high heat-transfer rates typical

of nucleate boiling have, in the main, been attributed to bubble-induced agitation near the heating surface. This has lead to correlation equations of the general form:

$$Nu = \text{const. } Re^m \, . \, Pr^n \tag{3}$$

where the dimensionless parameters are evaluated in terms of bubble characteristics. The better known of these have recently been reviewed by Zuber and Fried [5].

At a particular pressure and for a given surface–liquid combination these reduce approximately to:

$$(q/A) = \text{const. } (\Delta T_{\text{sat}})^a \tag{4}$$

Clearly since the nucleation characteristics of the heating surface are ignored, such equations cannot adequately correlate nucleate boiling data. Attempts to accommodate nucleation effects by the inclusion of active site concentration terms have lead to equations of the form [6–9]:

$$(q/A) = \text{const. } N^b \, (\Delta T_{\text{sat}})^c \tag{5}$$

Inasmuch as these relations do not take account of latent heat transport, N represents the number of liquid flow-inducing sources.

Recent indirect evidence [10–12], however, suggests that latent heat transport cannot be ignored in saturated boiling. Irrespective of the heat-transfer mechanism operating in nucleate boiling, a study of the parameters entering into equation (2), as well as their inter-relation, would appear to be necessary.

In our reports of 1960 [13, 14] attempts at the photographic determination of N, f and V_d and at the evaluation of latent heat transport in saturated boiling were reported. It was shown that for water and ethyl alcohol boiling at atmospheric pressure latent heat transport increases steadily with increasing flux, until in the vicinity of the peak flux it alone accounts for the total flux. At no stage was its contribution negligible. Due to shortcomings of the photographic technique the bubble volume at departure could not be accurately determined. Also, bubble frequencies could only be measured at relatively low fluxes, high-flux values being obtained by extrapolation using an empirical equation fitted to the low-flux data. Thus there was some doubt as to the accuracy of the latent heat transport determination. The main conclusions reached are, however, still considered valid.

1.3 *Purpose and outline of this study*

Summarizing then: One is faced with a situation in which every better known heat-transfer correlation for saturated nucleate boiling is based on the experimentally unverified assumption that the contribution to the total flux by latent heat transport is negligible. Recent work indicates that this concept is almost certainly incorrect.

In this paper determinations of latent heat transport in saturated boiling of water at atmospheric pressure are reported. Further investigations into the basic parameters entering into the latent heat transport equation, that is equation (2), are presented.

In Section 2 experimental work on latent heat transport is described. Section 3 deals with bubble frequencies and bubble volumes at departure and their inter-relation. Section 4 provides data on the concentration of bubble producing sites and is a study of nucleation.

2. CONTRIBUTION TO THE TOTAL FLUX BY LATENT HEAT TRANSPORT

2.1 *Apparatus and measuring technique*

The apparatus used permitted determination of the heat flux and temperature difference between the heating surface and the liquid bulk; a means of measuring N, f and V_d was also provided.

Boiling vessel (*Fig.* 1). This contained a horizontal, electrically heated nickel wire, 0·02 in dia., which acted both as a heating element and as a resistance thermometer. (A wire rather than a flat plate was used because of the greater ease in interpreting the resultant photographs. Also edge effects were thereby avoided.) An auxiliary heater maintained the liquid bulk at the saturation temperature corresponding to ambient atmospheric pressure ($\simeq$12 psia). A mercury-in-glass thermometer measured the liquid bulk temperature. The test wire was placed in an inner tank. This has been shown to be necessary if stagnant pool conditions are to be maintained in the test

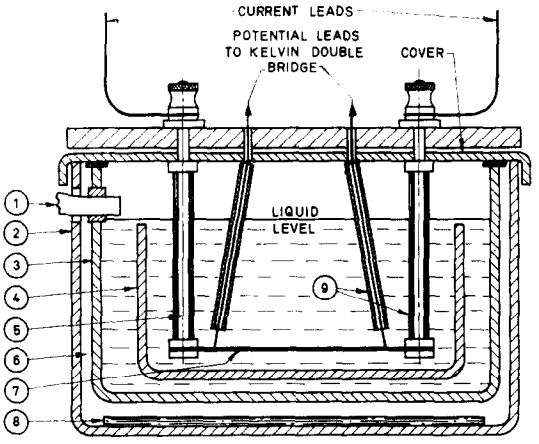

—LEGEND—
1 TO CONDENSING SYSTEM
2 OUTER TANK
3 MIDDLE TANK
4 CONVECTION TANK
5 MOUNTING POSTS
6 AIR SPACE
7 TEST WIRE
8 AUXILIARY HEATER
9 GLASS INSULATING SLEEVES

FIG. 1. Boiling vessel.

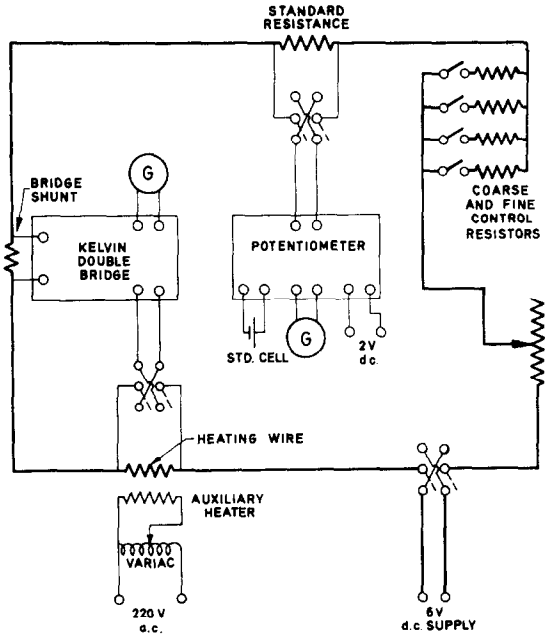

FIG. 2. Heating and measuring circuit diagram.

liquid [15]; its omission results in variation of the heat transfer from the wire with the power level of the auxiliary heater.

The whole system was completely sealed off from the atmosphere thus ensuring utmost cleanliness during testing.

Electrical system (*Fig.* 2). The wire resistance was measured by means of a Kelvin double bridge, whereas the heating current was determined from the volt-drop across a standard resistance in series with the heating wire.

Photographic technique. This consisted of taking a fixed number of successive photographs of the test section and bubble field. A variable-speed drum camera, provided with a commutator for triggering a flashing light source, was used. Timing marks were provided by a neon-lamp. The control circuit used is shown diagrammatically in Fig. 3. With this system 16 successive frames could be obtained, a

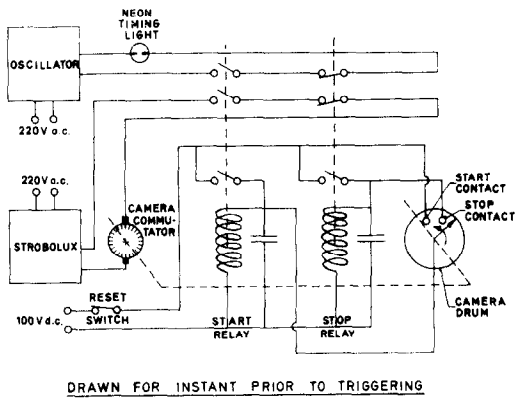

FIG. 3. Photography control circuit.

taking speed of about 85 frames/s being generally used. This allowed at least one cycle of the low frequency bubbles to appear on each loop. Specimen photographs are shown in Fig. 4.

2.2 *Test procedure*

After thorough cleaning the boiling tank was filled with the test liquid—de-ionized water. De-aeration of the liquid and the heating surface was effected by high-flux boiling for approximately 6 h.

The test proper was then commenced. Measurement of the wire resistance and the potential drop over the standard resistor were

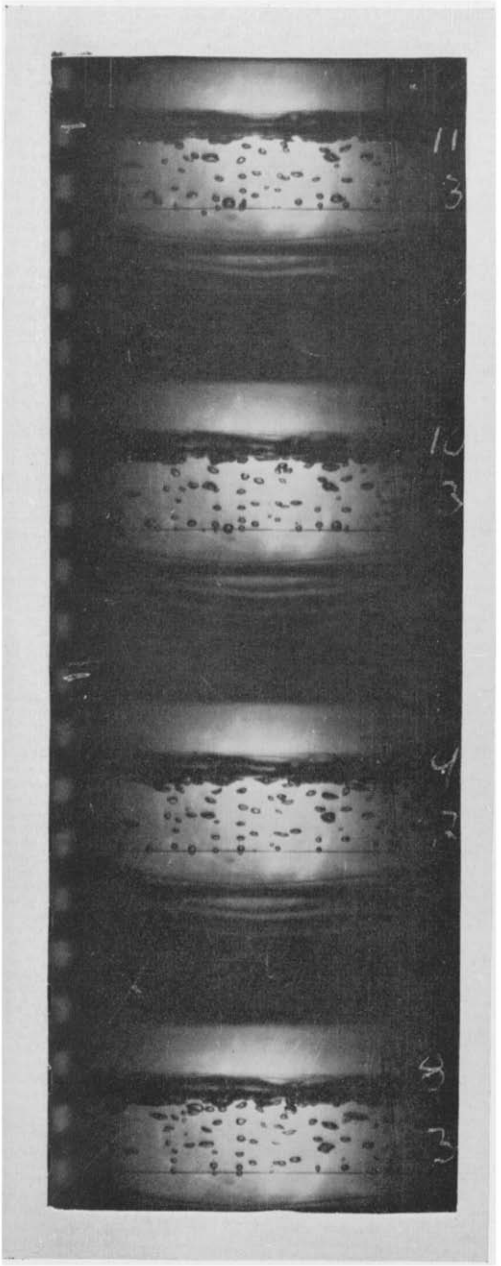

FIG. 4(a). Specimen photograph. Film loop 3 $(q/A) = 38{\cdot}6 \times 10^3$ Btu/h ft^2.

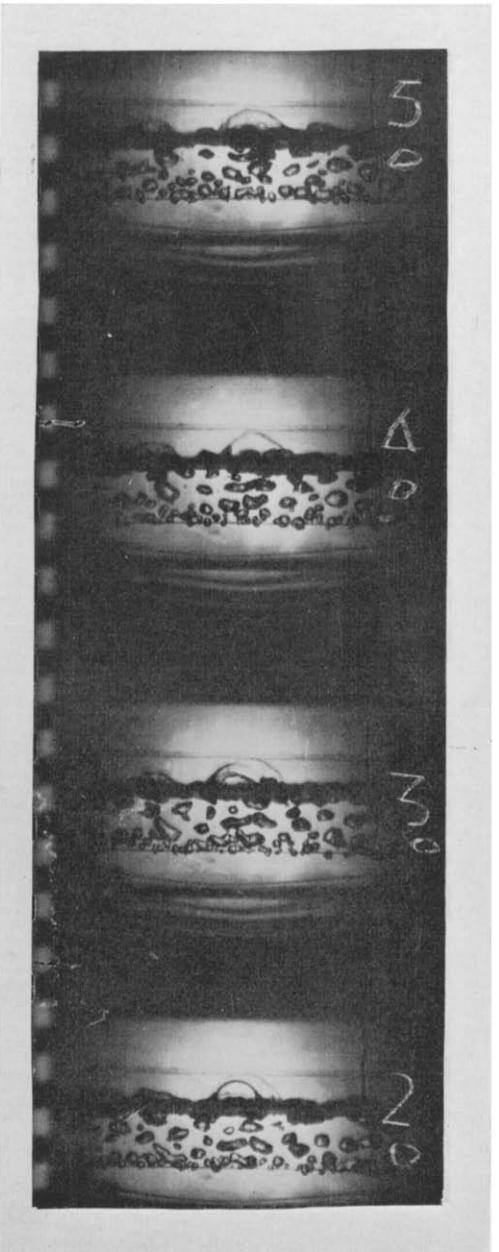

FIG. 4(b). Specimen photograph. Film loop 0 $(q/A) = 157 \times 10^3$ Btu/h ft^2.

taken. A loop of film was exposed in the manner described above. This procedure was repeated at progressively lower fluxes, some four to five minutes being allowed for conditions to settle after each change in heating current. Determination of the boiling curve with flux progressively decreasing has been shown by several workers to give the most reproducible results. Measurements were extended into the region of natural convection.

2.3 *Computations, errors and interpretation of photographs*

Heat fluxes and temperature differences (wire surface to liquid bulk) were calculated from electrical and thermometric measurements. Kok [15] using this apparatus, estimated the maximum error in heat flux determinations as ± 1 per cent and the error in the temperature difference as ± 5 per cent under worst conditions.

The negatives of the film loops obtained were examined under magnification by projecting them onto a screen. Bubble sources, frequencies and volumes at departure were determined.

At low fluxes the number of bubble sources could be counted with ease [see Fig. 4(a)]. At higher fluxes adjacent growing bubbles coalesced to form larger vapour globules [see Fig. 4(b)].†

The photographs of Séméria [16, 17] and Gaertner [11] clearly show large vapour globules attached to the heating surface by several stems. Such large globules are made up of vapour emanating from several nucleation sites. Bubble volume at departure can only be defined as the volume of a vapour globule leaving the surface, irrespective of whether the globule arises from one or more nucleation sites. Thus to maintain the meaning of equation (2), N, the number of bubble sources per unit area, must be defined as the number of regions per unit area from which vapour globules emanate, irrespective of whether such regions contain one or more nucleation sites. At low flux in the region of isolated bubbles the bubble source concentration equals the nucleation site concentration; after bubble coalescence this relation ceases to hold. The error in determining N is roughly the same as that in the measurement of the heating surface area, that is ± 1 per cent.

Preliminary tests conducted at various camera speeds showed that, with the optimum speed of approximately 85 frames/s used, the maximum error in determining the bubble frequency is about ± 2 per cent.

Because of the relatively low camera speed it was rarely possible to obtain a photograph of a bubble at the instant of departure. Jakob [3], however, has found that at about the time of departure a bubble grows relatively slowly. Figure 5 shows three bubble-volume vs time

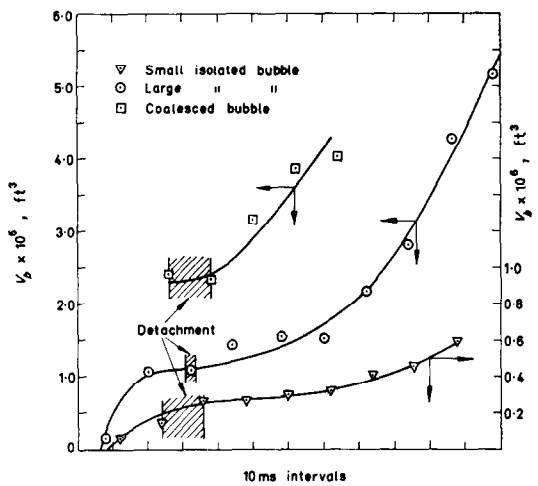

FIG. 5. Bubble growth curves.

curves determined with the apparatus described above. For all three types of bubble considered the growth curves flatten out in the vicinity of departure. The instant of departure was caught only for the large isolated bubble. Thus the first picture showing a bubble detached can be satisfactorily used for the determination of bubble volume at departure, whenever departure is not photographed; this procedure was adopted throughout.

Bubble volumes were calculated on the assumption that bubbles are spheroids. At low flux this assumption holds well; at high flux its validity is dubious. For this and other reasons measurements were not extended to very high fluxes.

† Evidently the flux at which discrete bubbles or globules occur is much higher with thin wires than with flat plates [11, 18, 19]. Continuous vapour columns or jets were not observed even at the highest heat flux investigated, 157 000 Btu/h ft².

When bubble dimensions were measured under magnification some error was introduced due to blurring of the outlines. The resulting error in bubble volume is estimated at ± 20 per cent for the smallest bubbles observed and less than ± 5 per cent for the largest. Taking bubble size distribution into account, this leads to an error in latent heat transport of ± 8 per cent at both the highest and the lowest heat fluxes measured.

The overall error in the determination of latent heat transport may thus be taken as ± 12 per cent.

2.4 *Results and discussion*

The boiling curve, log (q/A) vs ΔT_{sat}, and the latent heat transport, as calculated from equation (2), are plotted in Fig. 6. The natural convection data are correlated and extrapolated by an equation of the form $(q/A)_{NC} = C\Delta T_{sat}^{5/4}$

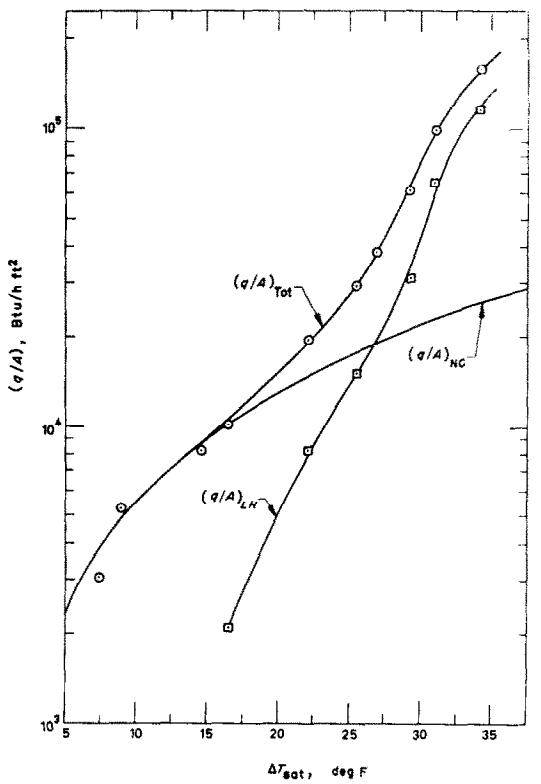

FIG. 6. Boiling curve for water also showing latent heat transport and extrapolated natural convection curve.

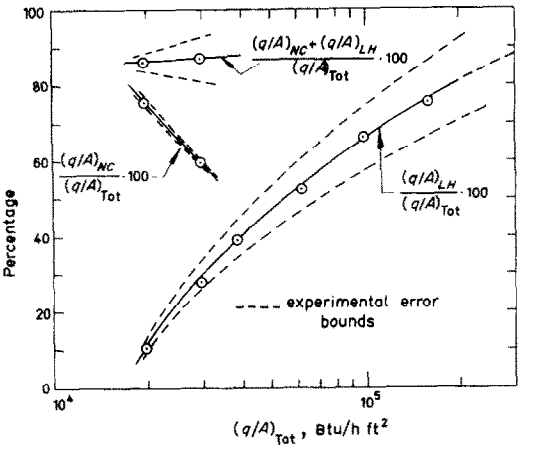

FIG. 7. Latent heat transport and convection as percentages of total heat flux.

[13, 14]. The percentage contribution of latent heat transport to the total flux is plotted against $(q/A)_{Tot}$ in Fig. 7. Clearly this contribution is nowhere insignificant.

The error-bounds on Fig. 7 are based on values of ± 12 per cent in latent heat transport and ± 1 per cent in total flux. Evidently the latent heat transport contribution increases smoothly with flux; at the peak flux (not determined in this study but generally in the vicinity of 4 to 6 $\times$ 10^5 Btu/h ft^2) it alone might represent the total flux. It is also noteworthy that the relation

$$(q/A)_{LH} = \text{const.}\,(q/A)_{Tot} \qquad (6)$$

stated or implied in several studies does not hold.

It was stated earlier that latent heat transport and convection (natural and bubble-induced) are the predominant mechanisms operative during saturated boiling. Other possible mechanisms, e.g. mass transfer through bubbles, were considered negligible. The following substantiates this view: Hsu and Graham [20] have shown that, with respect to thermal boundary layer disturbance, the area of influence of one bubble source is small and corresponds to about two bubble diameters. It seems reasonable to assume therefore that in the region of very low bubble-source concentration the *convection* mechanism from a heating surface may be

approximated by one of undisturbed *natural convection*. Thus for the first two determinations at low flux the percentage convection contribution (obtained from extrapolated natural convection data) is plotted in Fig. 7. The sum of the percentage latent heat contribution and the percentage convection contribution is very nearly 100 per cent within the estimated error bounds. It is felt that the small discrepancy shown is due to the neglect of bubble-induced flow.

3. RELATION BETWEEN BUBBLE FREQUENCY AND BUBBLE VOLUME AT DEPARTURE

3.1 *Review of previous work*

The product of bubble frequency, f, and bubble diameter† (or bubble volume) at departure, D_d, enters into many analyses of nucleate boiling and also into the expression for latent heat transport, equation (2). As such the interrelation between frequency and diameter at departure has been the subject of several investigations, both analytical and experimental. A brief survey of these is given here.

Jakob and Linke [21] and Fritz and Ende [22] presented the first experimental studies of bubble detachment. In the limited flux range investigated mean frequencies and bubble diameters at departure were found to be independent of flux. Thus the product of mean diameter, $\bar{D}_d$, and mean frequency, $\bar{f}$, was a constant, that is, at a particular pressure

$$\bar{D}_d \,.\, \bar{f} = \text{const.} \tag{7}$$

More recently Perkins and Westwater [23] presented a similar study for the medium and high flux boiling of methanol. They found that for fluxes up to 80 per cent of the peak flux the mean frequencies and mean departure diameters remained constant; hence their product was also a constant.

The same result was obtained by Yamagata *et al.* [18] for the boiling of water in the region of isolated bubbles. After the onset of coalescence the data showed a larger scatter.

In the region of the peak heat flux an analysis by Deissler [24] suggests the relation between mean departure diameter and frequency as

$$\bar{D}_d^{0.5} \bar{f} = \text{const.} \tag{8}$$

Cole [25] was able to obtain some experimental substantiation of Deissler's analysis.

A recent analysis by McFadden and Grassmann [26] also leads to equation (8) and is supported by limited data on the boiling of liquid nitrogen.

Zuber [27] has proposed an equation yielding the product of mean bubble frequency and mean departure diameter in terms of physical properties of liquid and vapour.

$$\bar{D}_d \bar{f} = 0{\cdot}59\,[\sigma g(\rho_L - \rho_v)/\rho_L^2]^{0.25} \tag{9}$$

At constant pressure this relation reduces to Jakob's equation (7).

The following section considers the significance of these results.

3.2 *Definition of mean bubble frequency and mean bubble volume (or diameter) at departure*

The purpose of studying bubble frequencies and volumes at departure, as well as their product, is the obtention of the mass velocity of bubbles leaving the heating surface.

Consider a heating surface of area A having n bubble producing sites of individual frequencies f_i and individual bubble volumes at departure V_{di}, where $i = 1, 2, \ldots, n$. The fundamental definition of the mass velocity of departing bubbles, G_d, is

$$G_d = \sum_{i=1}^{n} (f_i\, V_{di})\, \rho_v / A \tag{10}$$

G_d can also be expressed in terms of mean frequencies and volumes such that

$$G_d = (n/A)\bar{f} \,.\, \bar{V}_d\, \rho_v = \sum_{i=1}^{n} (f_i\, V_{di})\, \rho_v / A \tag{11}$$

The left-hand side of equation (11) is the generally used, though not fundamental, definition of the mass velocity of departing bubbles.

It is the general practice to substitute into the left-hand side of equation (11) the *arithmetic* means of bubble frequencies and departure volumes in an attempt to obtain G_d. This procedure is clearly invalid [28].

† For non-spherical bubbles defined as equivalent spherical diameter.

Evidently equation (11) permits any definition of one of the parameters $\bar{f}$ or $\bar{V}_d$; the definition of the other is then fixed. Thus, for example, if we define mean bubble volume at departure as the arithmetic mean of bubble volumes over all sources, that is,

$$\bar{V}_d = \sum_{i=1}^{n} V_{di}/n \tag{12a}$$

then the necessary definition of mean frequency follows from equation (11) as

$$\bar{f} = \sum_{i=1}^{n} (f_i\ V_{di}) / \sum_{i=1}^{n} V_{di} \tag{12b}$$

For purposes of obtaining the mass velocity it is unnecessary to separate the product $f\,V_d$ into $\bar{f}$ and $\bar{V}_d$. We therefore define the mean of the product of frequency and departure volume as

$$\overline{f\,V_d} = \sum_{i=1}^{n} (f_i\ V_{di})/n \tag{13}$$

and G_d as,

$$G_d = (n/A)\overline{f\,V_d}\ \rho_v = \sum_{i=1}^{n} (f_j\ V_{di})\ \rho_v/A \tag{14}$$

Equation (13) is consistent with the two expressions for G_d in equation (14).

3.3 *Expected behaviour of $f_i\ V_{di}$ and $\overline{f\,V_d}$*

For a constant flux from a heating surface, it is possible to produce various arguments which suggest that at any particular surface temperature the product $f_i\ V_{di}$ should be the same for all sources. Consider, for example, the following: A bubble in growing extracts heat from the thermal boundary layer and in departing leaves behind an area of destroyed boundary layer [20, 29]. Bubbles of large departure volumes will cause large areas of destruction. Now bubble frequency is determined by the waiting period (the time required for the recovery of the boundary layer) and by the bubble growth period. The waiting period and the growth period are generally of comparable magnitude. A large area of destruction will have a long waiting period and a large departure volume will require a long growth period. Thus a large departure volume is associated with a low frequency and vice-versa. This description is oversimplified—see for example [20]; however it does suggest the possibility of an interrelation of the type

$$f_i\ V_{di} = \text{const.} \tag{15}$$

where $i = 1, 2, \ldots, n$, and n is the number of bubble sources. Some statistical scatter is to be expected.

Dealing now with the variation of the mean product $\overline{f\,V_d}$ with flux (or temperature difference) the definition of latent heat transport is recalled

$$(q/A)_{LH} = N\overline{f\,V_d}\ \lambda_v\ \rho_v \tag{16}$$

N and $\overline{f\,V_d}$ are the only terms that vary with flux. If $(q/A)_{LH}$ and N are plotted against $(q/A)_{\text{Tot}}$ an idea of the variation of $\overline{f\,V_d}$ can be obtained from the slopes. In Fig. 8 the data of the present study are represented in this fashion. The N vs $(q/A)_{\text{Tot}}$ curve will be discussed in Section 4. It is immediately clear that $\overline{f\,V_d}$ cannot be independent of flux since the slopes of these curves are not equal; also that $\overline{f\,V_d}$ should increase slowly at first and more rapidly

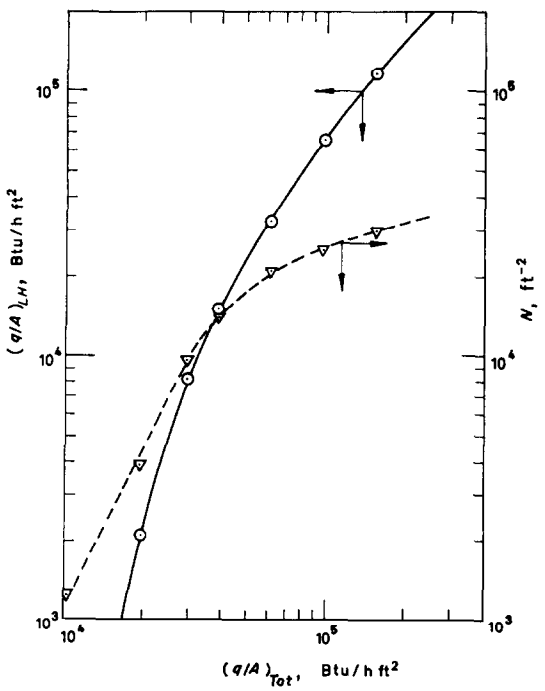

FIG. 8. Latent heat transport and bubble source concentration versus total heat flux, showing difference in slopes.

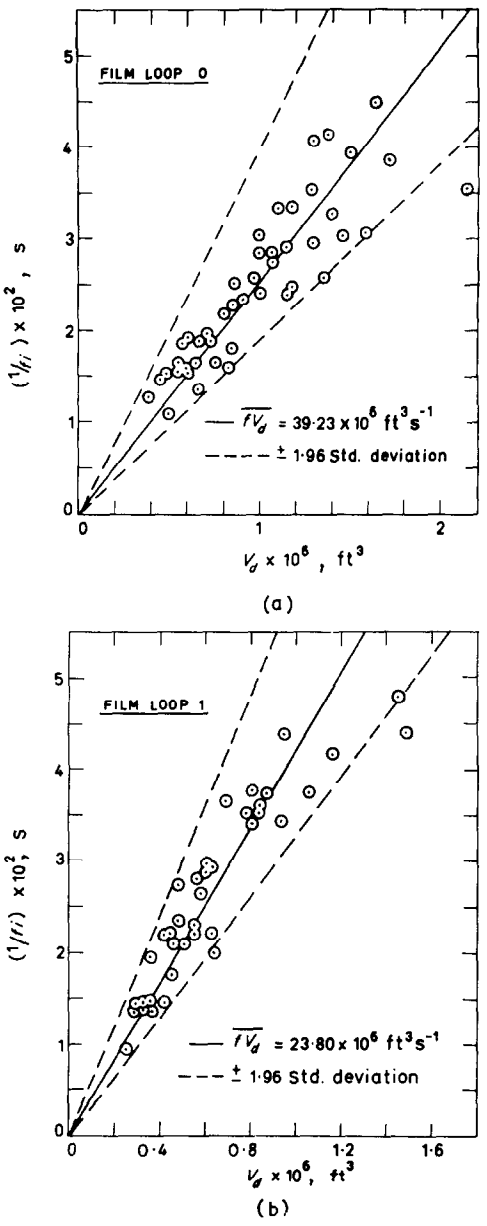

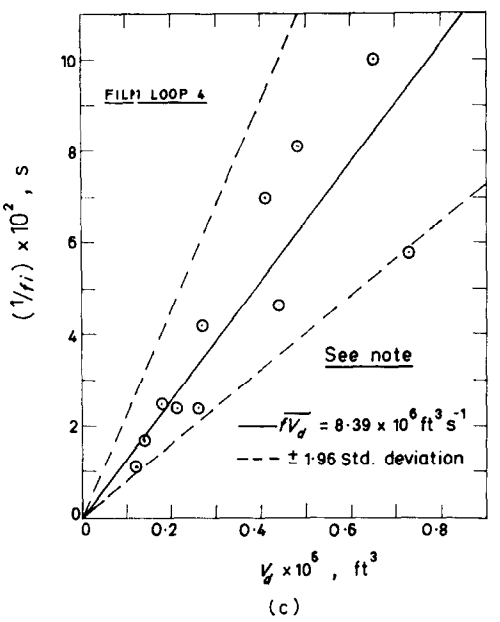

FIG. 9. Relationship between bubble frequency and volume at departure. *Note:* In (c) two bubbles of large volume and unmeasured frequency are not shown. For latent heat transport purposes their contribution was included by estimating their frequency from $\overline{fV_d}$.

as the flux (or the temperature difference) increases.

3.4. *Experimental results and discussion*

The product $f_i V_{di}$. For purposes of testing the hypothesis that at a particular flux $f_i V_{di}$ = const. it is convenient to write this relation as

$$V_{di} = \text{const.}\ (1/f_i) \qquad (17)$$

Thus when plotting V_{di} against $(1/f_i)$ a straight line through the origin is obtained if the hypothesis holds. In Fig. 9 three sets of data, two at high flux and one at low flux, are shown. The full line on each represents the arithmetic mean of the products $f_i V_{di}$, that is $\overline{fV_d}$, at that flux. Similar plots were obtained for all six film loops exposed, with the data of loop 5 (at the lowest flux) showing a much higher scatter. Thus the proposed relation, equation (15) or (17) holds within certain scatter limits.

It is of interest to determine the correlation coefficient for V_{di} and $(1/f_i)$ for the six tests. A correlation coefficient, r, may be computed for any two-dimensional set of observations, but unless the underlying population is two-dimensionally normally distributed the interpretation of r is uncertain. Thus only if both V_{di} and $(1/f_i)$ are normally distributed for a set of observations can the correlation coefficient be regarded as a measure of their interrelation, with $|r| = 1$ indicating linear dependence [30].

For the observations here reported the distributions of V_{di} and $(1/f_i)$ were generally not normal. However, the departure from normality was not large, especially for the data at higher fluxes. As an example, Fig. 10 shows the

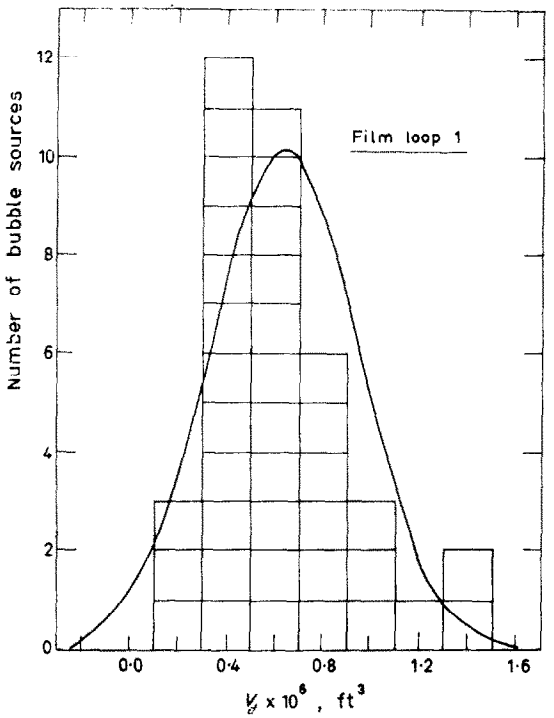

FIG. 10. Histogram of departure volumes (film loop 1) with superimposed normal distribution.

histogram of V_{di} for film loop 1 compared with the normal distribution of mean and variance equal to that of the histogram. Thus some significance may be attached to the correlation coefficients for the tests here reported.

The coefficients obtained ranged from 0·83 to 0·92 for film loops 0 to 4, with loop 5 at the lowest flux yielding 0·67. This represents significant support for the hypothesis that at a particular flux (which is not too low) the volumetric vapour flow rate is the same from each source.

Consider the scatter in the values of the product $f_i V_{di}$ at a particular flux. At low fluxes where bubble formation frequently occurs in bursts this scatter is to be expected. Difficulties in measuring bubble volumes, especially after the onset of coalescence, have also been mentioned. In addition, because of the limited number of frames in each loop, it was necessary to assume that at any flux successive bubble periods and departure volumes from a particular source were equal. Hsu and Graham [20], when studying the ebullition cycle from a single source during steady boiling, found large variations in both waiting and growth periods. The variation of their sum, the bubble period $(=1/f_i)$ was less but still significant. Unfortunately the film loops of the tests reported here were not sufficiently long to allow a reasonable determination of f_i and V_{di} values where each is an average over a period of time from a particular source. This is probably responsible for most of the observed scatter.

The product $\overline{f V_d}$. The variation of the product $\overline{f V_d}$ with both flux and ΔT_{sat} is shown in Fig. 11.

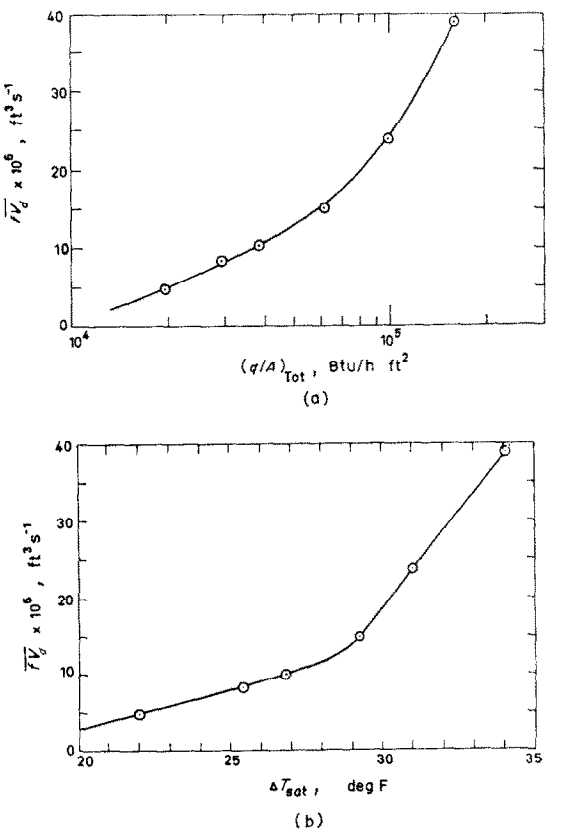

FIG. 11. Variation of mean product of bubble frequency and departure volume with (a) heat flux and (b) wall superheat.

As anticipated from Fig. 8 this product is not constant. The "knee" in Fig. 11(b) is associated with the onset of coalescence.

4. NUCLEATION SITES AND BUBBLE SOURCES

4.1 *Preliminary consideration and predictions*

Effect of temperature difference. Nucleation proceeds from surface cavities of certain geometry [31, 32, 33, 34]. The mean mouth size of these cavities will in general be distributed in some way—for argument's sake as in Fig. 12.

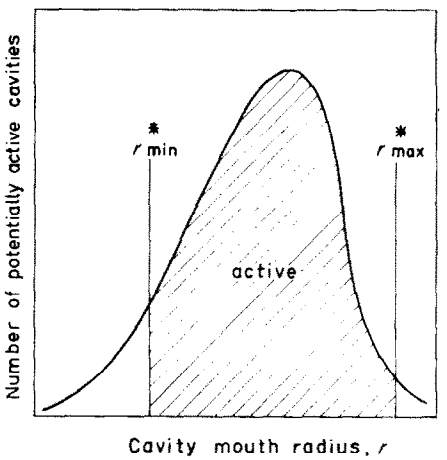

FIG. 12. Hypothetical size-distribution of nucleation cavities.

Under given conditions a particular size range of these cavities will be active. The size of the largest active cavity, r^*_{max}, may be boundary-layer controlled; the size of the smallest active cavity, r^*_{min}, is thermodynamically controlled.

For the time being consideration is limited to "smooth" surfaces, that is, to conditions such that the largest cavity present on the surface (of mouth radius r_{max}) is always active that is,

$$r^*_{max} = r_{max} = \text{const.} \tag{18a}$$

This is equivalent to saying that the limiting thermal boundary-layer thicknesses, δ, which is flux and pressure dependent, must at all stages be great enough to contain the vapour nucleus from the largest cavity, that is,

$$\delta \geqslant r_{max} \tag{18b}$$

Nucleation may be then characterized to a reasonable approximation [11, 57] by

$$r^*_{min} = 2\sigma T_{sat}\, v_v/\lambda_v \Delta T_{sat} \tag{19}$$

Now it is recalled that in the study of Griffith and Wallis [33] it was shown that an equation virtually identical to equation (19) did not hold for artificial cavities punched into a surface from which boiling took place. It appears, however, that with the relatively large cavity size employed ($r = 2{\cdot}7 \times 10^{-3}$ in) the situation arose where $r > \delta$. Thus the punched cavities were not active at all and smaller natural cavities led to superheats higher than those predicted. In a constant temperature field [33] and under conditions where the limitation of equation (18) was satisfied [35] equation (19) did hold.

At constant pressure and with physical properties evaluated at the saturation temperature equation (19) reduces to

$$r^*_{min} = \text{const.}/\Delta T_{sat} \tag{20}$$

Thus the rate of change of the active cavity (nucleation site) concentration with ΔT_{sat}—$d\mathcal{N}/d(\Delta T_{sat})$—may be drawn against ΔT_{sat} as in Fig. 13(a), that is, approximately as the lateral inversion of the cavity size distribution of Fig. 12.

Consider now a liquid at saturation temperature and events accompanying a gradual raising of the wall superheat, ΔT_{sat}. At a temperature difference $(\Delta T_{sat})_{min}$ the first cavity of radius r_{max} is activated. As ΔT_{sat} is raised, smaller cavities become active and the nucleation site concentration, $\mathcal{N}$, on the surface increases. Figure 13(b) shows the variation of $\mathcal{N}$ with ΔT_{sat}, that is, the cumulative distribution corresponding to that of Fig. 13(a). At some point, say A, bubble coalescence on the surface will commence. It now becomes necessary to distinguish between the nucleation site concentration $\mathcal{N}$ and the bubble source concentration, N. In the interval $\Delta(\Delta T_{sat})$, $\Delta\mathcal{N}$ cavities are activated. If bubbles growing from these were all to coalesce with already existing bubbles then the N versus ΔT_{sat} curve would branch out horizontally to point B in Fig. 13(b). This is an extreme case. In actual fact only a fraction, say x, of $\Delta\mathcal{N}$ will be lost as bubble sources. At the onset of coalescence x is expected to be small; thus the N vs ΔT_{sat} curve moves to point A'. x will be higher in each interval of progressively greater ΔT_{sat}. Thus the N vs ΔT_{sat} curve will take the shape shown in Fig.

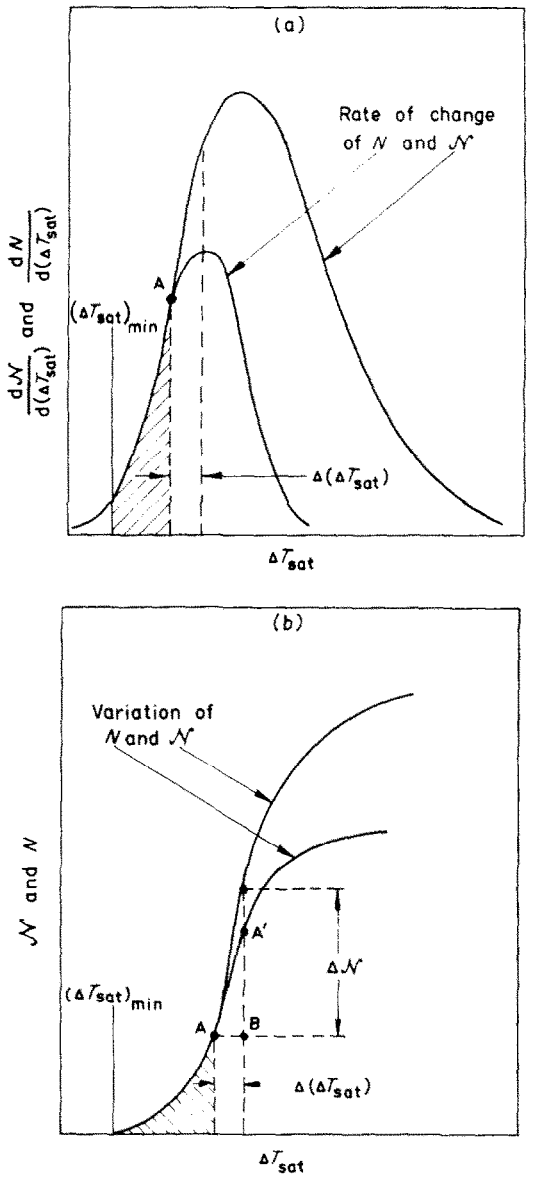

FIG. 13. Hypothetical bubble population: (a) Rate of change of nucleation site ($\mathcal{N}$) and bubble source (N) concentrations with wall superheat (ΔT_{sat}) (b) $\mathcal{N}$ and N vs ΔT_{sat}.

13(b). This curve represents the integration of the distribution $dN/d(\Delta T_{sat})$ versus ΔT_{sat} shown in Fig. 13(a).

Consideration was originally limited to systems where r^*_{max} is independent of flux and ΔT_{sat}. This imposed the condition that the relation $\delta \geqslant r_{max}$ must hold at all stages. Depending on the micro-roughness of a surface this condition may or may not be satisfied. If it is not then r^*_{max} is boundary-layer controlled. The limiting boundary-layer thickness is expected to decrease with increasing flux and ΔT_{sat} [16]. Thus with sufficiently rough surfaces r^*_{max} will decrease with increasing ΔT_{sat}. This would cause a lowering of the N versus ΔT_{sat} curve. In the coalescence regime the decrease in N due to this effect might well be compensated by a corresponding reduction in coalescence. Unfortunately no quantitative information on δ and its variation with flux, in the vicinity of a bubble source, is available.

Whatever the surface, the experimentally obtainable N versus ΔT_{sat} curve is expected to assume the shape of some cumulative frequency distribution. This might not be readily recognizable, especially if available data cover a limited range only. Differentiation and plotting of the $dN/d(\Delta T_{sat})$ versus ΔT_{sat} distribution should yield more information.

In Section 4.2 experimental data will be examined in the light of these predictions.

The effect of pressure. Séméria [16] has pointed out that the effect of pressure on equation (19) is such as to permit the use of

$$r^*_{min} = \text{const.}/\Delta T_{sat} \cdot P_L \qquad (21)$$

for water in the pressure range 1 to 50 atm. This relation is also applicable, to a rougher approximation, to several other substances if P_L is substantially below their critical pressure (see Fig. 14).

Thus if the pressure is reduced on a boiling system r^*_{min} increases. During operation at some low pressure the situation will arise where $r^*_{min} = r^*_{max}$, that is, where the size range of active cavities is zero. Nucleation, and hence nucleate boiling, must then be expected to cease, or otherwise to proceed by some mechanism other than the normal. It is seen from equation (21) that this critical situation may be reached (at some low pressure) in the middle of a boiling curve as ΔT_{sat} is progressively lowered. At some even lower pressure the ΔT_{sat} required for normal nucleation is greater than that associated with the peak flux; below

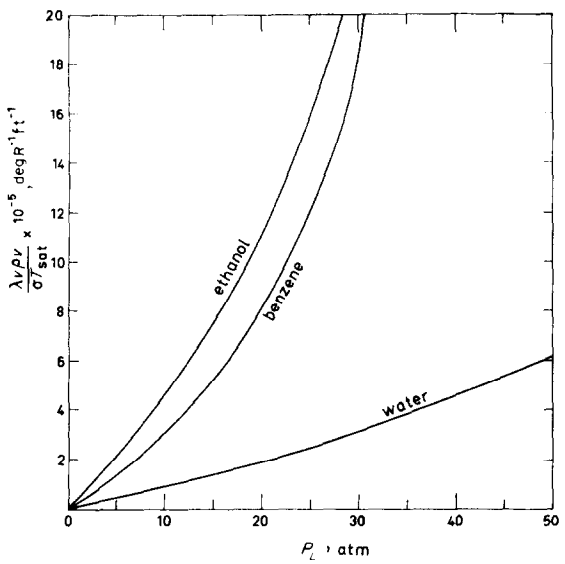

FIG. 14. Variation of $\lambda_v \rho_v / \sigma T_{sat}$ with pressure [see equations (19) and (21)].

this pressure the normal nucleate regime is altogether absent.

In Section 4.2 experimental work aimed at the verification of these predictions is reported.

4.2 *Experimental work and discussion*

Effect of temperature difference and flux. In Fig. 15 the data of the present study are handled in the manner suggested in Section 4.1. These results appear to support the proposed hypothesis surprisingly well. The fact that the distributions N vs ΔT_{sat} and $dN/d(\Delta T_{sat})$ vs ΔT_{sat} roughly approximate to normal is of no particular significance and arises from the micro-structure of the heating surface employed. In fact, other data [15] which were analysed in this fashion showed these trends less clearly. However, the approach appears to be potentially valuable. Before significant advances can be made along these lines more quantitative information on coalescence must be obtained. Séméria [16, 17] has recognized this necessity.

Bubble sources and flux. It is more common to present data on bubble source concentration as log (q/A) vs log N plots. In Fig. 16 data of the present study are plotted in this manner. In addition, data on low pressure boiling of ethanol and benzene [35] are also given. These data were obtained by visual counting with an apparatus very similar to the one described earlier, but allowing pressure variations. The heating wire diameter was 0·0076 in.

In the low and intermediate flux range the relationship

$$(q/A)_{Tot} = \text{const. } N^{0.5} \qquad (22)$$

proposed by several workers evidently holds. At higher fluxes however, N increases more slowly with flux, with the index reaching 2·6 for for the water data. The visual data on organics could not be extended to sufficiently high fluxes. The "knees" of the curves correspond to the onset of coalescence.

Effect of pressure. The predictions of Section 4.1 suggest the necessity of conducting boiling runs [(q/A) decreasing] at various low pressures with a particular surface–liquid combination. Such tests were performed [35] at saturation temperature, great care being taken to avoid the well-known "hysteresis" effect and to maintain

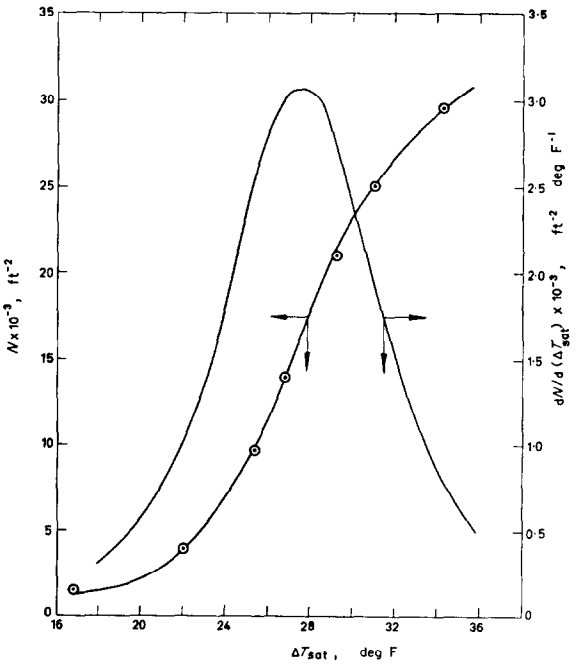

FIG. 15. Observed variation of bubble source concentration and its rate of change with wall superheat.

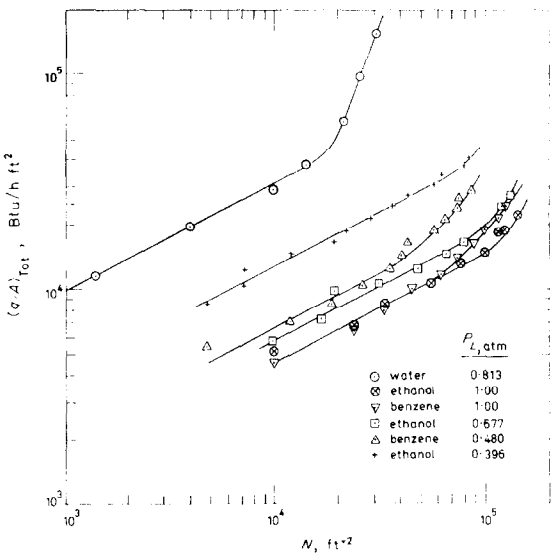

FIG. 16. Variation of bubble source concentration with heat flux.

reproducibility. Results obtained for ethanol are presented in Fig. 17.

During run E.1 (1·0 atm) and run E.2 (0·677 atm) the well-known boiling curves were traced. This also applies to run E.3 (0·396 atm) in the high flux range.

At low flux, run E.3 exhibits a highly unusual change in direction. This behaviour appears to be associated with the cessation of operation of the normal mechanism of nucleation. Inspection of Fig. 16 in which the N vs (q/A) data for this run are reported shows that no dramatic change in the bubble source concentration occurred at this point. However, nucleation seemed to become unstable; bubbles no longer emanated from fixed sources in column-formation, but appeared to be formed at points shifting on the surface. This effect was particularly noticeable in run E.4 (0·294 atm) where bubble-producing sources jumped around on

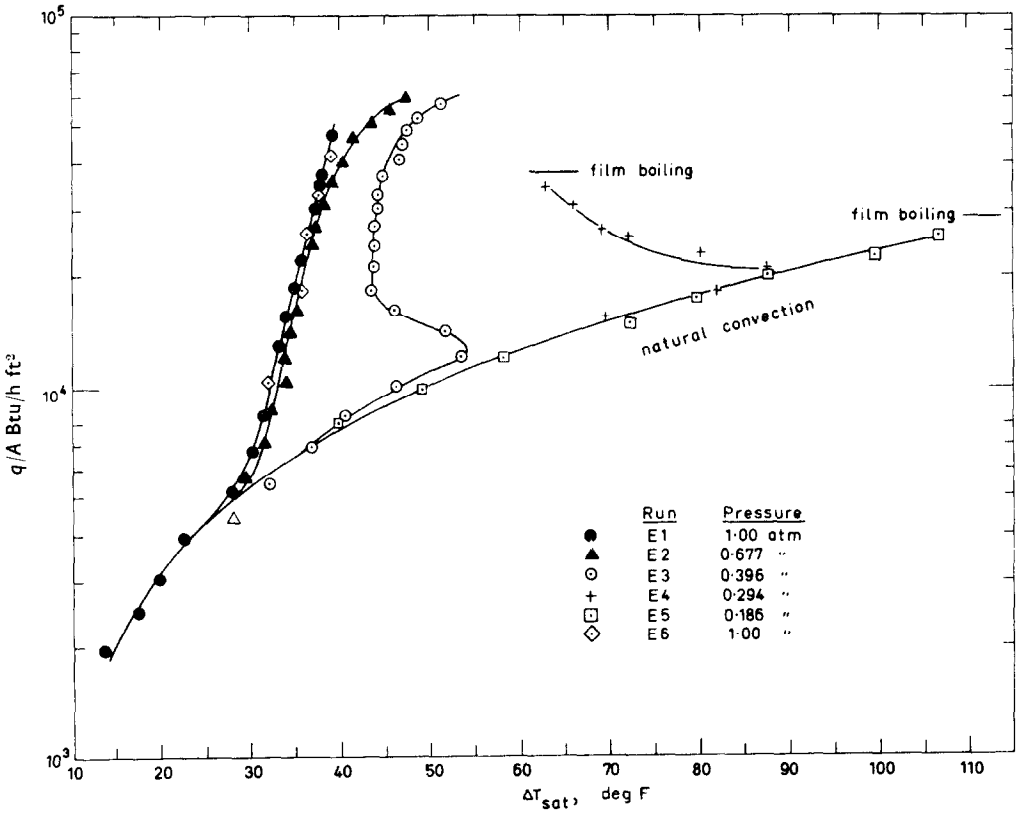

FIG. 17. Boiling curves for ethanol showing unstable nucleate boiling and absence of the nucleate regime at low pressure.

the surface in a rapid and apparently random manner. A curve of the shape of run E.3 has been obtained by van Stralen [36] for the boiling of a solution of whey in water at 0·132 atm pressure. Boiling as in run E.4 does not appear to have been hitherto reported.

The phenomena of runs E.3 and E.4 cannot be attributed to "hysteresis effects" or "temperature overshoot" since: (i) runs were performed at decreasing flux, (ii) the test procedure in obtaining runs E.3 and E.4 was identical to that adopted for the stable runs E.1 and E.2, and (iii) the behaviour did not die away with time; in fact on one occasion during operation in the unstable region the flux was maintained at the same setting for over an hour, but the bubble pattern remained irregular; in the same run at higher flux no irregularity was observed.

Run E.5 (0·136 atm) illustrates the complete cessation of nucleation. At a flux slightly higher than that of the last point recorded the surface burst into film boiling. The nucleate regime was entirely absent. Van Stralen [37] and Lienhard and Schrock [38] have observed the same phenomenon.

Run E.6 (1·0 atm) is a satisfactory check on reproducibility.

Similar results to the above were obtained for benzene, bromobenzene, *n*-hexanol and both mixed and pure isomers of xylene.

The predictions of Section 4.1 thus appear to be verified. At some low pressure the cessation of nucleation by the normal mechanism occurs. This can take place in the middle of a boiling curve. A hitherto unrecognized regime of unstable nucleate boiling exists at low pressure. At even lower pressure the nucleate regime is altogether absent.

For the case where the limitation of equation (18) is obeyed it appears possible to predict the onset of the unstable boiling region [57]. This will be fully dealt with elsewhere.

The cessation-of-nucleation phenomenon has been known for many years in the guise of "bumping". Generations of organic chemists performing "vacuum-distillations" in glass apparatus have added anything from chunks of coal to talcum powder [39] in an effort to prevent these minor explosions. Sometimes these devices were helpful, sometimes not, depending upon whether they did or did not provide the nucleation sites previously absent.

It is felt that low pressure work of the type described above is potentially an extremely powerful tool in the general study of nucleation.

5. CONCLUSIONS

(1) Latent heat transport and convection together account for the total flux in saturated nucleate boiling.

(2) Latent heat transport is at stages significant; it is probable that at burnout it alone represents the total flux.

(3) The mean product of bubble frequency and departure volume, $\overline{fV_d}$, *if correctly defined*, increases throughout the flux range.

(4) At fixed flux and pressure the product fV_d is the same for each bubble source within reasonable statistical scatter.

(5) The relationship between heat flux (q/A) and number of bubble sources per unit area, N,

$$(q/A) = \text{const. } N^n$$

where $n \simeq 0{\cdot}5$ holds only in the absence of coalescence.

(6) It appears possible to determine the *size distribution* of potential nucleation cavities on a surface if the following are available:

(a) The distribution of $\mathrm{d}N/\mathrm{d}(\Delta T_{\mathrm{sat}})$ vs ΔT_{sat} together with data on coalescence, thus allowing the determination of the $\mathrm{d}\mathcal{N}/\mathrm{d}(\Delta T_{\mathrm{sat}})$ vs ΔT_{sat} distribution.

(b) A criterion of nucleation in non-uniform fields.

(7) The approximate equation

$$r^*_{\mathrm{min}} = 2\sigma T_{\mathrm{sat}}\, v_v/\lambda_v\, \Delta T_{\mathrm{sat}}$$

being a necessary but not sufficient criterion of nucleation under boiling conditions can, however, yield predictions on the size range of nucleation cavities. These have been verified by experiments and lead to the following general conclusions:

(a) The effect of lowering the pressure on a boiling system is such as to decrease the size range of active cavities.

(b) For a particular surface–liquid combination a particular low pressure exists below which the boiling curve exhibits instability.

(c) This threshold is reached when the size range of cavities active in the normal sense becomes zero. Beyond this threshold there exists a hitherto unrecognized regime of unstable nucleate boiling. In this unstable regime nucleation and boiling proceed by mechanisms other than the normal. At even lower pressures the nucleate regime is altogether absent.

ACKNOWLEDGEMENTS

Messrs. S. Hyman and D. J. Carliell assisted in obtaining data on water.

Thanks are extended to the South African Council for Scientific and Industrial Research for their faith in financially supporting this programme over the years.

H. H. Jawurek at present holds a bursary from the South African Atomic Energy Board. He was formerly supported by a junior lectureship at the University of Cape Town, Department of Chemical Engineering, to whose Head, Dr. A. D. Carr, sincere thanks are offered.

REFERENCES

1. W. M. Rohsenow and J. A. Clark, A study of the mechanism of boiling heat transfer, *Trans. Amer. Soc. Mech. Engrs* **73**, 609–620 (1951).
2. R. F. Larson, contribution to ref. 1.
3. M. Jakob, *Heat Transfer*, Vol. 1, p. 634. John Wiley, New York (1949).
4. F. C. Gunther and F. Kreith, Photographic study of bubble formation in heat transfer to subcooled water, *Heat Transfer and Fluid Mechanics Institute*, p. 113–138. ASME (1949).
5. N. Zuber and E. Fried, Two phase flow and boiling heat transfer to cryogenic liquids, *J. Amer. Rocket Soc.* **32**, 1332–1341 (1962).
6. H. M. Kurihara and J. E. Myers, The effects of superheat and surface roughness on boiling coefficients, *J. Amer. Inst. Chem. Engrs* **6**, 83–91 (1960).
7. N. Zuber, Hydrodynamic aspects of nucleate pool boiling, Ramo-Wooldridge Research Laboratory Report, *RW-RL*-164 (1960).
8. C. L. Tien, A hydrodynamic model for nucleate pool boiling, *Int. J. Heat Mass Transfer* **5**, 533–540 (1962).
9. J. H. Lienhard, A semi-rational nucleate boiling heat flux correlation, *Int. J. Heat Mass Transfer* **6**, 216–219 (1963).
10. F. D. Moore and R. B. Mesler, The measurement of rapid surface temperature fluctuations during nucleate boiling of water, *J. Amer. Inst. Chem. Engrs* **7**, 620–624 (1961).
11. R. F. Gaertner, Photographic study of nucleate pool boiling on a horizontal surface. General Electric Co. Research Laboratory Report 63-*RL*-3357*C*, Schenectady, N.Y. (1963).
12. S. G. Bankoff, A note on latent heat transport in nucleate boiling, *J. Amer. Inst. Chem. Engrs* **8**, 63–65 (1962).
13. C. J. Rallis, R. V. Greenland and A. Kok, Stagnant pool boiling from horizontal wires under saturated and sub-cooled conditions, *S. Afr. Mech. Engr* **10**, 171–186 (1961).
14. R. V. Greenland, An investigation into stagnant pool nucleate boiling from horizontal wires for saturated and sub-cooled conditions. *M.Sc. Thesis* in Mech. Engng, Univ. of the Witwatersrand, Johannesburg, S. Africa (1960).
15. A. Kok, An experimental investigation of nucleate boiling heat transfer under stagnant pool conditions. *M.Sc. Thesis* in Mech. Engng, Univ. of the Witwatersrand, Johannesburg, S. Africa (1960).
16. R. L. Séméria, Quelques résultats sur le méchanisme de l'ébullition. *VIIèmes Journées de l'Hydraulique, Soc. Hydrotechnique de France*, Question II, Rapport No. 3, Paris (1962).
17. R. L. Séméria, An experimental study of the characteristics of vapour bubbles, Paper 7, *Symposium of Two-phase Fluid Flow*, Inst. Mech. Engrs, London (1962).
18. K. Yamagata, F. Hirano, K. Nishikawa and H. Matsuoka, Nucleate boiling of water on the horizontal heating surface. *Mem. Fac. Engng, Kyushu* **15**, No. 1, 99–163 (1955).
19. B. J. Stock, Observations on transition boiling heat transfer phenomena. Argonne National Lab. Report *ANL*-6175, Argonne, Ill. (1960).
20. Y. Y. Hsu and R. W. Graham, An analytical and experimental study of the thermal boundary layer and ebullition cycle in nucleate boiling. *NASA TN-D*-594, Lewis Research Centre, Cleveland, Ohio (1961).
21. M. Jakob and W. Linke, Der Wärmeübergang von einer waagerechten Platte an siedendes Wasser, *Forsch. Geb. Ing.* **4**, 75 (1933).
22. W. Fritz and W. Ende, Über den Verdampfungsvorgang nach kinematographischen Aufnahmen an Dampfblasen, *Phys. Z.* **37**, 391–401 (1936).
23. H. S. Perkins and J. W. Westwater, Measurements of bubbles formed in boiling methanol, *J. Amer. Inst. Chem. Engrs* **2**, 471–476 (1956).
24. R. G. Deissler, *Columbia Heat Transfer Symp.*, New York (1954). Cited in ref. 49.
25. R. Cole, A photographic study of pool boiling in the region of the critical heat flux, *J. Amer. Inst. Chem. Engrs* **6**, 533–538 (1960).
26. P. W. McFadden and P. Grassmann, The relation between bubble frequency and diameter during nucleate pool boiling, *Int. J. Heat Mass Transfer* **5**, 169–173 (1962).
27. N. Zuber, Hydrodynamic aspects of boiling heat transfer. U.S. Atomic Energy Commission Rep. *AECU*-4439, AEC Tech. Inf. Serv., Oak Ridge, Tenn. (1959).

28. H. H. JAWUREK, The definition of mean bubble frequency and mean bubble volume at departure in nucleate boiling, *S. Afr. Mech. Engrs* **13**, 47–48 (1963).
29. Y. Y. HSU, On the size range of active nucleation cavities on a heating surface, *J. Heat Transfer* **C84**, 207–219 (1962).
30. A. HALD, *Statistical Theory with Engineering Applications*, Chapter 19, section 13. John Wiley, New York (1952).
31. S. G. BANKOFF, Ebullition from solid surfaces in the absence of a pre-existing gaseous phase, *Trans. Amer. Soc. Mech. Engrs* **79**, 735–740 (1957).
32. H. B. CLARK, P. S. STRENGE and J. W. WESTWATER, Active sites for nucleate boiling, *Chem. Engng Progr. Symp.* Ser. **55**, No. 29, 103–110 (1959).
33. P. GRIFFITH and J. D. WALLIS, The role of surface conditions in nucleate boiling, *Chem. Engng Progr. Symp.* Ser. **56**, No. 30, 49–65 (1960).
34. S. G. BANKOFF, Entrapment of gas in the spreading of a liquid over a rough surface, *J. Amer. Inst. Chem. Engrs* **4**, 24–26 (1958).
35. H. H. JAWUREK, Nucleation during boiling with special reference to its cessation at low pressure. *M.Sc. Thesis* in Chem. Engng, University of Cape Town, Rondebosch, S. Africa (1962).
36. S. J. D. VAN STRALEN, Heat transfer to boiling binary liquid mixtures, Part III, *Brit. Chem. Engng* **6**, 834 (1961).
37. S. J. D. VAN STRALEN, Heat transfer to boiling binary liquid mixtures at atmospheric and sub-atmospheric pressures, *Chem. Engng Sci.* **5**, 290–296 (1956).
38. J. H. LIENHARD and V. E. SCHROCK, The effect of pressure, geometry and the equation of state upon the peak and minimum boiling heat flux, *J. Heat Transfer* **C85**, 261–272 (1963).
39. J. W. WESTWATER, *Advances in Chemical Engineering*, Vol. 2 (Edited by T. B. DREW and J. W. HOOPER), pp. 27–29. Academic Press, New York (1953).

Résumé—Un travail expérimental sur l'ébullition par germes dans un réservoir d'eau saturée est exposé. Celui-ci indique que le transport de chaleur latente, $(q/A)_{LH}$ est important à toutes les étapes. Le rapport $(q/A)_{LH}/(q/A)_{Tot}$ croît régulièrement lorsque le flux de chaleur croît et semble tendre vers l'unité lorsque $(q/A)_{Tot}$ tend vers les conditions de caléfaction. Le transport de chaleur latente et la convection rendent compte du flux total dans l'ébullition saturée.

Les paramètres de base entrant dans la formulation $(q/A)_{LH}$, c'est-à-dire le produit de la fréquence des bulles et du volume initial des bulles $f V_d$, et la concentration des sources de bulles N, sont étudiés plus profondément.

On montre que la plupart des découvertes publiées sur le paramètre $f V_d$ est inapplicable aux corrélations, ceci étant dû à la définition incorrecte des moyennes. Les résultats expérimentaux montrent que (i) le produit moyen (arithmétique) $\overline{f V_d}$ croît avec le flux, et (ii) que pour un flux particulier le produit $f V_d$ est approximativement le même pour chaque source de bulle.

Les données pour N dans l'ébullition de l'eau et des liquides organiques à différentes pressions indiquent que la relation

$$(q/A) = \text{Constante } N^n$$

où $n \simeq 0{,}5$ semble s'appliquer seulement dans la région des bulles isolées.

Une hypothèse est développée et confirmée expérimentalement selon laquelle la courbe donnant N en fonction de ΔT_{sat} prend la forme d'une distribution de fréquence cumulée.

L'analyse et des expériences de confirmation montrent que la nucléation et l'ébullition par germes ne peuvent pas se produire indéfiniment à des pressions de plus en plus basses; pour une combinaison particulière surface-liquide il existe une pression qui marque le seuil d'un régime inconnu jusqu'à présent d'ébullition instable par germes. A des pressions plus faibles, le régime par germes est entièrement absent.

Zusammenfassung—Es wird über experimentelle Arbeiten beim Blasensieden in freier Konvektion in Wasser vom Sättigungszustand berichtet. Dabei erweist sich der Transport latenter Wärme $(q/A)_{LH}$ in allen Stufen als bedeutsam. Das Verhältnis $(q/A)_{LH}/(q/A)_{Tot}$ nimmt mit wachsender Wärmestromdichte dauernd zu und scheint dem Wert eins zuzustreben, wenn sich $(q/A)_{Tot}$ dem burn-out Punkt nähert. Der Transport latenter Wärme zusammen mit der Konvektion bedingt den gesamten Wärmestrom beim Sieden in der Flüssigkeit von Sättigungszustand. Die für die Bestimmung von $(q/A)_{LH}$ notwendigen Grundparameter nämlich das Produkt aus Blasenfrequenz und Blasenvolumen beim Abreissen $f V_d$ und die Anzahl der Blasenkeime N werden weiter untersucht.

Es wird gezeigt, dass die meisten über den Parameter $f V_d$ veröffentlichten Ergebnisse, wegen der ungenauen Definition der Mittelwerte, auf die Wärmeübergangsbeziehungen nicht anwendbar sind. Die Versuchsergebnisse zeigen, dass (i) das (arithmetische) mittlere Produkt $\overline{f V_d}$ mit der Stromdichte zunimmt und (ii) ab einer besonderen Stromdichte das Produkt $f V_d$ für jede Wärmequelle etwa dasselbe ist.

Die Daten für N bei Wasser und organischen Flüssigkeiten die bei verschiedenen Drücken sieden, zeigen, dass die Beziehung

$$(q/A) = \text{constant } N^n$$

mit $n \simeq 0{,}5$ nur im Bereich von Einzelblasen zu gelten scheint.

Eine Hypothese wurde entwickelt und experimentell bestätigt; Danach nimmt die Kurve von N über ΔT_{sat} die Form einer kumulativen Frequenzverteilung an.

Die Analyse und Kontrollversuche zeigen, dass Keimbildung und Blasensieden bei kleiner werdenden Drücken nicht unbegrenzt gesteigert werden können. Für eine bestimmte Oberflächen–Flüssigkeitskombination existiert ein Druck der den Grenzwert markiert für ein bisher unbekanntes Regime des nichtstabilen Blasensiedens. Bei kleineren Drücken tritt das Blasenregime überhaupt nicht auf.

Аннотация—Рассматривается экспериментальная работа по пузырьковому кипению с открытой поверхности воды в состоянии насыщения. Она подтверждает, что перенос скрытой теплоты, $(q/A)_{LH}$, значителен во всех стадиях. Найдено, что отношение $(q/A)_{LH}/(q/A)_{\text{Tot}}$ равномерно возрастает с увеличением теплового потока, и что оно стремится к единице по мере того как величина $(q/A)_{\text{Tot}}$ стремится к критической. Как перенос скрытой теплоты, так и конвекция существенны для суммарной величины теплового потока при насыщенном кипении. Проводится дальнейшее исследование основных параметров, входящих в выражение, описывающее $(q/A)_{LH}$—произведения частоты пузырьков и объема пузырьков fV_d и концентрации источников пузырьков N.

Показано, что большинство опубликованных данных по параметру fV_d неприменимо к соотношениям теплообмена в связи с неправильным проведением усреднений. Результаты эксперимента показывают, что: (1) среднеарифметическое произведение $\overline{fV_d}$ увеличивается по мере возрастания теплового потока, и (2) при определенном тепловом потоке произведение fV_d примерно одинаково для каждого источника пузырьков.

Данные значений величины N при кипении воды и органических веществ при различных давлениях показывают, что соотношение

$$(q/A) = \text{constant } N^n$$

где $n \simeq 0{,}5$ справедливо только для области изолированных пузырьков. Развита и экспериментально подтверждена гипотеза, согласно которой кривая зависимости N от ΔT_{sat} принимает вид интегральной кривой распределения частоты.

Анализ и подтверждающие его эксперименты показывают, что невозможно сделать так, чтобы образование пузырьков и пузырьковое кипение продолжалось неограниченно при все понижающихся давлениях; для определенной комбинации поверхность-жидкость имеет место давление, которое характеризует порог наступления до настоящего времени неизвестного режима неустойчивого пузырькового кипения. При низких давлениях пузырьковый режим полностью отсутствует.